Inhibition of extracellular signal-regulated kinase downregulates endoplasmic reticulum stress-induced apoptosis and decreases brain injury in a cardiac arrest rat model

Zhang-Li Yuan[1,*]; Zong-Xiang Zhang[2,*]; Yan-Zi Mo[3]; De-Li Li[4]; Lu Xie[4]; Meng-Hua Chen[3]

[1] Department of Emergency Medicine, The Second Affiliated Hospital of Guangxi Medical University, Nanning, Guangxi 530007, People's Republic of China.

[2] Intensive Care Unit, Wuming Hospital of Guangxi Medical University, Nanning, Guangxi 530199, People's Republic of China

[3] Intensive Care Unit, The Second Affiliated Hospital of Guangxi Medical University, Nanning, Guangxi 530007, People's Republic of China

[4] Department of Physiology, Guangxi Medical University, Nanning, Guangxi 530021, People's Republic of China

[*] These authors contributed equally to this work

Corresponding authors:

Meng-Hua Chen, xyicucmh@sina.com; 166 Daxuedong Road, Nanning, Guangxi, People's Republic of China, 530007

Lu Xie, xielu8282@163.com; 22 Shuangyong Road, Nanning, Guangxi, People's Republic of China, 530021

Short title: ERK regulates ERs-induced apoptosis after CIRI

Summary

Cerebral ischemia-reperfusion injury (CIRI) is the predominant cause of neurological disability after cardiac arrest/cardiopulmonary resuscitation (CA/CPR). The endoplasmic reticulum stress (ERs)-induced apoptosis plays an important role in neuronal survival/death in CIRI. Our previous studies reported that the extracellular signal-regulated kinase (ERK) inhibitor, PD98059, alleviates CIRI after CA/CPR. Whether ERs-induced apoptosis is involved in the neuroprotection of PD98059 remains unknown. This study aims to investigate the effects of ERK inhibition by PD98059 on ERs-induced apoptosis after CIRI in the CA/CPR rat model. The baseline characteristics of male adult Sprague-Dawley (SD) rats in all groups were evaluated before CA/CPR. The SD rats that survived from CA/CPR were randomly divided into 3 groups (n = 12/group): normal saline group (1 ml/kg), Dimethylsulfoxide (DMSO, the solvent of PD98059, 1 ml/kg) group, PD98059 group (0.3 mg/kg). Another 12 SD rats were randomly selected as the Sham group. Twenty-four hours after resuscitation, neural injury was assessed by survival rate, neurological deficit scores (NDS) and Nissl staining; apoptosis of brain cells was detected using terminal deoxynucleotidyl transferase dUTP nick end labeling (TUNEL) staining; mRNA expression and protein levels of ERs-related protein BIP, PERK, ATF4 and CHOP were checked with RT-PCR and Western Blot. The results showed that there were no significant differences in baseline characteristics before CA/CPR among all groups. PD98059 significantly improved survival rate and NDS, increased the Nissl bodies in neurons, reduced

apoptosis, downregulated the mRNA transcription and expression levels of BIP, PERK, ATF4 and CHOP at 24 h after CA/CPR. Our results demonstrate that inhibition of ERK by PD98059 alleviates ERs-induced apoptosis via BIP-PERK-ATF4-CHOP signaling pathway and mitigates CIRI in the CA/CPR rat model.

1. Introduction

Cardiac arrest (CA) is a major global public health problem with high incidence and low survival rate. The most effective treatment is rapid initiation of cardiopulmonary resuscitation (CPR) to achieve return of spontaneous circulation (ROSC). However, CA/CPR inevitably leads to cerebral ischemia-reperfusion injury (CIRI), which is the major cause of neurological disability and death. There are few available effective treatments for CIRI in patients after ROSC except for the target temperature management [1]. Further elucidation of the pathophysiological mechanisms is a prerequisite for improving the therapeutic strategies for CIRI [2,3].

Previous studies have showed that the dysfunction of endoplasmic reticulum (ER) is involved in the pathogenesis of CIRI. ER plays an important role in regulating protein synthesis, folding, and degradation [4]. Under pathological conditions, the balance between protein loading and folding is broken, leading to the accumulation of unfolded or misfolded proteins in ER lumen, known as ER stress (ERs) [5]. To cope with ERs,

unfolded protein response (UPR) mediated by three ER transmembrane protein sensors - protein kinase RNA-like ER kinase (PERK), activated transcription factor 6 (ATF6) and inositol requiring enzyme 1 (IRE1) - is activated to restore ER homeostasis. In resting cell, PERK, ATF6 and IRE1 are held inactive by the binding of chaperone binding immunoglobulin protein (BIP). Upon ERs, these sensors dissociate from BIP and trig three UPR signaling pathway to reduce protein synthesis, to increase protein folding and to accelerate degradation of misfolded proteins. The UPR is generally considered as a defensive mechanism when ERs is mild. However, when ERs is overactivated or prolonged, apoptosis can be initiated by the activation of the C/EBP homologous protein (CHOP), which is the converge for the three signaling pathways of UPR and a master regulator of ERs-induced apoptosis [6]. As a key sensor of ERs, PERK upregulates the expression of CHOP via increasing the translation of activated transcription factor 4 (ATF4) [7]. ERs-induced apoptosis mediated by PERK-ATF4-CHOP pathway is implicated in CIRI [8]. Regulation of ERs-induced apoptosis is crucial for neuronal survival/death and may be a potential therapeutic target.

Extracellular signal-regulated kinase (ERK) belongs to the family of mitogen-activated protein kinases (MAPKs) and regulates the pathogenesis in various human diseases [9]. The effect of ERK on ERs was determined by several evidences [10-12]. Our previous studies found that ERK inhibitor, PD98059, reduces brain injury and improves survival rate through reversing oxidative stress, mitochondrial pathway-mediated apoptosis and autophagy in CA/CPR rats [13,14]. However, it remains unknown whether alleviation of ERs-induced apoptosis is associated with the neuroprotection of ERK

inhibition. We hypothesized that inhibition of ERK mitigates ERs-induced apoptosis via PERK-ATF4-CHOP pathway. Accordingly, in this study, we aimed to examine the effect of ERK inhibitor, PD98059, on ERs-induced apoptosis and to explore its underlying mechanism involving PERK-ATF4-CHOP signaling pathway after CIRI in the CA/CPR rat model. We supposed that it may provide a novel insight into the therapy of CIRI.

2. Materials and Methods

2.1 Animals and experimental groups

The healthy male Sprague-Dawley (SD) rats (weight 200 - 230 g, age 6 - 8 weeks) were obtained from the experimental animal center of Guangxi Medical University. The animal experimentation was complied with the Guide for the Care and Use of Laboratory Animals (1985), NIH, Bethesda. This study was approved by the Animal Ethics Committee and the Animal Care Committee of Guangxi Medical University.

A total of 36 rats suffering from CA/CPR survived and were randomly divided into three groups ($n = 12$/group), including normal saline group (NS), intravenous injection of saline after ROSC; dimethylsulfoxide group (DMSO), intravenous injection of PD98059 solvent - DMSO after ROSC; and PD98059 group (PD), intravenous injection of PD98059 after ROSC. Another 12 healthy male rats were randomly selected as sham operation group (Sham).

2.2 The CA/CPR rat model

The CA/CPR model was performed according to the methods we previously published [15]. The pacing electrode connecting to the stimulator (Chengdu Technology

& Market Co. Ltd., China) was inserted orally and placed in the esophagus. Then the alternating current produced by the stimulator were delivered to the pacing electrode to induce ventricular fibrillation for 1 min. CPR was initiated after 7 min of CA with chest compression and mechanical ventilation (DH-150, the medical instrument of Zhejiang University, Hangzhou, China). ROSC was defined as mean arterial pressure (MAP) ≥ 50 mmHg accompanied by sinus, atrial, or borderline heart rhythm for more than 5 min. The rats not achieving ROSC in 3 min of CPR were excluded from the experiment.

2.3 Neurological function evaluation

Neurological deficits were assessed with the neurological deficit scores (NDS) according to the previous method [16] at 24 h after reperfusion. The score ranges from 0 to 80. A lower score corresponded to a more serious neurological deficit.

2.4 Preparation of brain tissues

All surviving rats were anesthetized with 2% pentobarbital (3 ml/kg) at 24 h after reperfusion. The brains of 6 rats from each group were harvested after tissue fixation with 4% paraformaldehyde, then sectioned at 4 μm for Nissl staining and TUNEL staining. The cerebral cortices of other 6 rats from each group were detached and frozen in a refrigerator (–80°C) immediately for PCR and Western Blot.

2.5 Nissl staining

Brain slices were stained with Nissl Staining Solution (G1430, Solarbio) for 30 min, dehydrated in 95% ethanol, cleared in dimethylbenzene, then covered with neutral balsam. The slices were observed under the pathology microscope (BX53+DP80, Olympus, Japan). The average optical density was used for the quantitative analysis of

Nissl body.

2.6 TUNEL staining

The terminal deoxynucleotidyl transferase dUTP nick end labeling (TUNEL) was used for detecting cell apoptosis. TUNEL staining was performed with In Situ Cell Death Detection Kit (11684817910, Roche, USA) according to the manufacturer's instruction. The slices were observed under the fluorescence microscopy (BX53 + DP80, Olympus, Japan). The apoptosis index = number of TUNEL (+) cell/number of total cells.

2.7 RT-PCR

The brain tissues samples (100 mg) were separated for extracting total RNA with Nucleozol (MNG, German). The concentration and purity of RNA were detected by UV spectrophotometer. The reverse transcription and amplification were performed with PrimeScript™ RT Master Mix (RR036A, Takara) and TB Green® Premix Ex Taq™ II (RR820A, Takara). The real-time PCR program was as follows: 95°C for 30sec; 40 cycles at 95°C for 5 sec, 60°C for 30 sec; and 95°C for 15 sec, 60°C for 1 min followed by 95°C for 15 sec. The primer sequences are as follows,

BIP-F: 5'-GCGAGTGTGAGAGGGAAGC-3'

BIP-R: 5'- CGCCGACGCAGGAGTA-3'

PERK-F: 5'-CCAGAGATTGAGACTGCGTG-3'

PERK-R: 5'-ATCTTATTCCCAAATACCTCTGGT-3'

ATF4-F: 5'- ATGTAGTTTTCTCTGCGCGT-3'

ATF4-R: 5'-TTAAATCGCTTCCCCCTTGG-3'

CHOP-F: 5'-ACCTGAGGAGAGAGTGTTCA-3'

CHOP-R: 5'-ACATCTGCAGGATAATGGGG-3'

GAPDH-F: 5'-CCGGGAAGGAAATGAATGGG-3'

GAPDH-R: 5'-GCCCAATACGACCAAATCAGAG-3'

2.8 Western Blot analysis

The brain tissues samples (40 mg) were lysed with RIPA buffer (R0010, Solarbio). The lysed protein was centrifuged at 12000 rpm for 20 min at 4℃. The supernatant was collected, and the total protein concentration was detected by the BCA Protein Assay Reagent Kit (AR1189, Boster, Wuhan, China). The protein samples (60 μg) were separated by 8% - 12% separation gel and then transferred to PVDF membranes (MERK&Co, NJ, USA). The PVDF membranes were incubated overnight at 4℃ with the primary antibodies included: BIP (3183S, CST), PERK (3192S, CST), ATF-4 (11815S, CST), CHOP (2895S, CST) and GAPDH (ab181602, Abcam). Then, the membranes were washed with Tris-buffered saline and incubated with the secondary antibody [anti-rabbit horseradish peroxidase-conjugated antibodies (Santa Cruz Biotechnology)] for 1 h. The proteins were detected using the chemiluminescent detection system (Gene Genius, India).

2.9 Statistical analysis

Statistical analyses were performed using SPSS 21.0 (IBM, Chicago, USA). Data were reported as mean ± standard deviation (SD). One-way analysis of variance (ANOVA) followed by least significance difference (LSD) post hoc test. The Chi-squared test was used to analyze survival rate. $P < 0.05$ was considered statistically

significant.

3. Results

3.1 Baseline Characteristics

The baseline parameters were as shown in Table 1, there were no significant differences in baseline characteristics before CA/CPR among all groups.

Table 1   Baseline parameters

Group	n	BW (g)	HR (beats/min)	SP (mmHg)	DP (mmHg)	MAP (mmHg)
Sham	12	330.96±13.62	414.75±11.66	119.33±4.85	99.00±4.81	109.17±4.17
NS	18	337.78±10.91	413.22±10.30	118.56±5.10	98.33±5.00	108.44±4.65
DMSO	18	334.56±15.10	410.22±10.30	117.72±4.35	100.44±4.57	110.50±4.59
PD	13	332.15±13.36	415.85+11.17	118.69±5.19	98.38±5.11	109.21±4.40

Sham, Sham-operated group; NS, saline group; DMSO, dimethyl sulfoxide group; PD, PD98059 group; BW, body weights; HR, heart rate; SP, systolic pressure; DP, diastolic pressure; MAP, mean arterial pressure. The values of baseline parameters are all represented as mean ± SD.

3.2 Inhibition of ERK improved the survival rate and NDS of rats at 24 h after reperfusion.

To investigate the effect of ERK inhibitor, PD98059, on the neurological function after CA/CPR, we first evaluated the survival rate and NDS. As shown in Table 2, the survival rate in the Sham group was 100%, which is significantly higher than that in the NS (67%) and DMSO (67%) groups ($P < 0.05$). The survival rate in the PD group (92%)

showed significant improvement compared with that in the DMSO group ($P < 0.05$).

No obvious neurologic deficit was observed in the Sham group at 24 h after CPR. In

contrast, severe neurological deficits were found in the NS and DMSO groups ($P <$

0.05). Administration of PD98059 significantly improved the NDS compared with that

in the DMSO group ($P < 0.05$). As expected, there was no significant difference of

survival rate and NDS between the NS and DMSO groups.

**Table 2**   Survival rate, CPR duration and NDS at 24 h after CPR

Group	Survival rate	n	CPR duration (s)	NDS
Sham	12/12(100%)	12	-	79.50±0.84
NS	12/18(67%) [#]	12	92.75±5.56	66.17±2.04 [#]
DMSO	12/18(67%) [#]	12	89.50±5.45	65.33±2.16 [#]
PD	12/13(92%) [&]	12	89.17±4.91	74.67±1.63 [&]

Sham, Sham-operated group; NS, saline group; DMSO, dimethyl sulfoxide group; PD, PD98059 group; CPR,

cardiopulmonary resuscitation; NDS, neurological deficit scores. The values of survival rate were represented as a

ratio. The values of CPR duration and NDS were represented as mean ± SD. #, $P < 0.05$ compared with the Sham

group; &, $P < 0.05$ compared with the DMSO group.

3.3 Inhibition of ERK increased the Nissl bodies in the cortices of rats at 24 h after

reperfusion.

To determine whether ERK inhibition by PD98059 protect the neurons from CIRI,

we observed the Nissl bodies in neurons with Nissl staining. As shown in Figure 1, the

neurons in the Sham group (A-a) were normal in structure and closely arranged with abundant distributed Nissl bodies, while the neurons in the NS (A-b) and DMSO (A-c) groups were loosely arranged and vacuolized in accompany with reduced Nissl bodies as evidenced by lower average optical density of Nissl bodies ($P < 0.05$). After administration with PD98059 (A-d), the neurons damage was mitigated as presented with higher average optical density of Nissl bodies compared with that in the DMSO groups ($P < 0.05$). There was no significant difference of average optical density of Nissl bodies between the NS and DMSO groups.
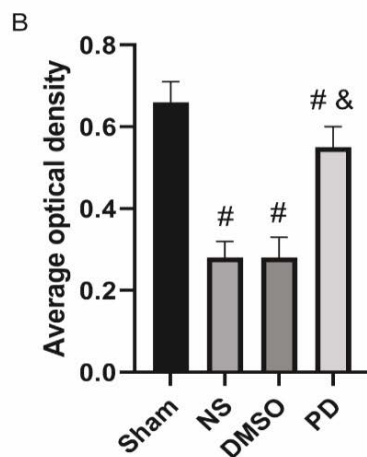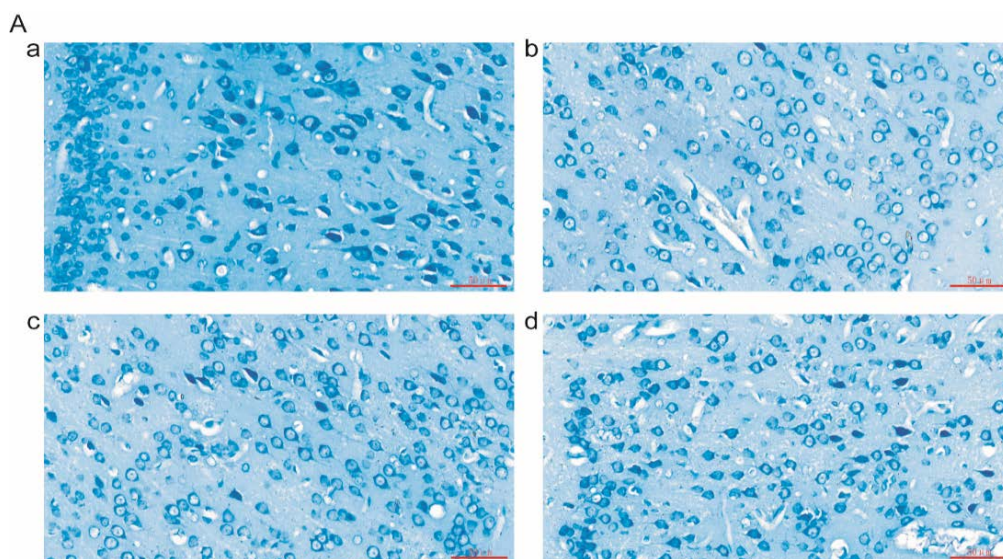
Figure 1   Inhibition of ERK increased the Nissl bodies in the cortices of rats at 24 h after reperfusion. (A) Nissl staining (blue) in the cortices of rats in the (A-a) sham, (A-b) NS, (A-c) DMSO and (A-d) PD groups. All images were represented with original magnification × 400. Scale bars = 50 μm. Sham, Sham-operated group; NS, saline group; DMSO, dimethyl sulfoxide group; PD, PD98059 group. (B) The optical density value of Nissl bodies was quantified by ImageJ 6.0 software. All data were represented as mean ± SD. #, $P < 0.05$ compared with the Sham group; &, $P < 0.05$ compared with the DMSO group.

3.4 Inhibition of ERK decreased neuronal apoptosis in the cortices of rats at 24 h after reperfusion.

The influence of ERK inhibition by PD98059 on neuronal apoptosis was tested using TUNEL and DAPI staining (as shown in Figure 2). The apoptotic index in the NS and DMSO groups was obviously higher than that in the Sham group ($P < 0.05$). The apoptosis index in the PD group was significantly lower than that in the DMSO group ($P < 0.05$). There was no significant difference of apoptotic index between the NS and DMSO groups.
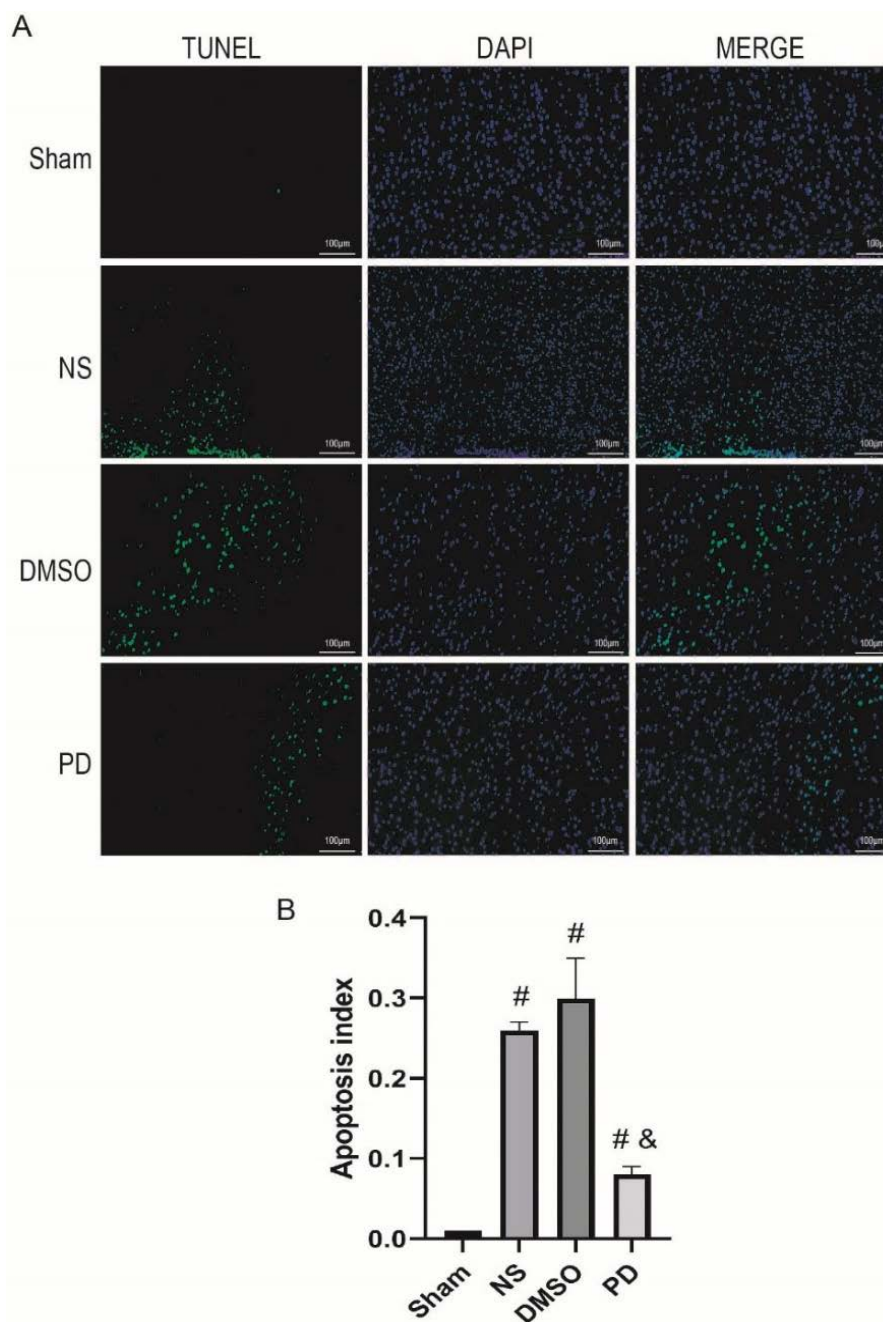
Figure 2 Inhibition of ERK reduced neuronal apoptosis in the cortices of rats at 24 h after reperfusion. (A) TUNEL

staining (green) was performed to reveal apoptosis cells; the nucleuses were stained with DAPI (blue). All images

were represented with original magnification × 200. Scale bars = 100 μm. Sham, Sham-operated group; NS, saline

group; DMSO, dimethyl sulfoxide group; PD, PD98059 group. (B) The apoptotic index was quantified by ImageJ

6.0 software. The values were expressed as the mean ± SD. #, $P < 0.05$ compared with the Sham group; &, $P < 0.05$

compared with the DMSO group.

3.5 Inhibition of ERK downregulated the mRNA transcription and expression levels of ERs-related proteins in the cortices of rat at 24 h after reperfusion.

To further explore whether the protective mechanism of PD98059 against ERs-induced apoptosis is involved in BIP-PERK-ATF4-CHOP pathway, we performed the RT- PCR and Western Blot to detect the mRNA transcription and expression levels of the ERs-related proteins BIP, PERK, ATF4 and CHOP after CA/CPR. As shown in Figure 3, the mRNA expression and the protein levels of BIP, PERK, ATF4, CHOP were detected. The mRNA expression of BIP (A-a), PERK (A-b), ATF4 (A-c) and CHOP (A-d) in the NS and DMSO groups were significantly increased than those in the Sham group ($P < 0.05$), and they were decreased in the PD group than that in the DMSO group ($P < 0.05$). The protein levels of BIP (B-a), PERK (B-b), ATF4 (B-c) and CHOP (B-d) in the NS and DMSO groups were significantly increased than those in the Sham group ($P < 0.05$), and the protein levels were decreased in the PD group than those in the DMSO group ($P < 0.05$). No significant difference was noted in the mRNA and protein expression levels of BIP, PERK, ATF4 and CHOP between the NS and DMSO groups.
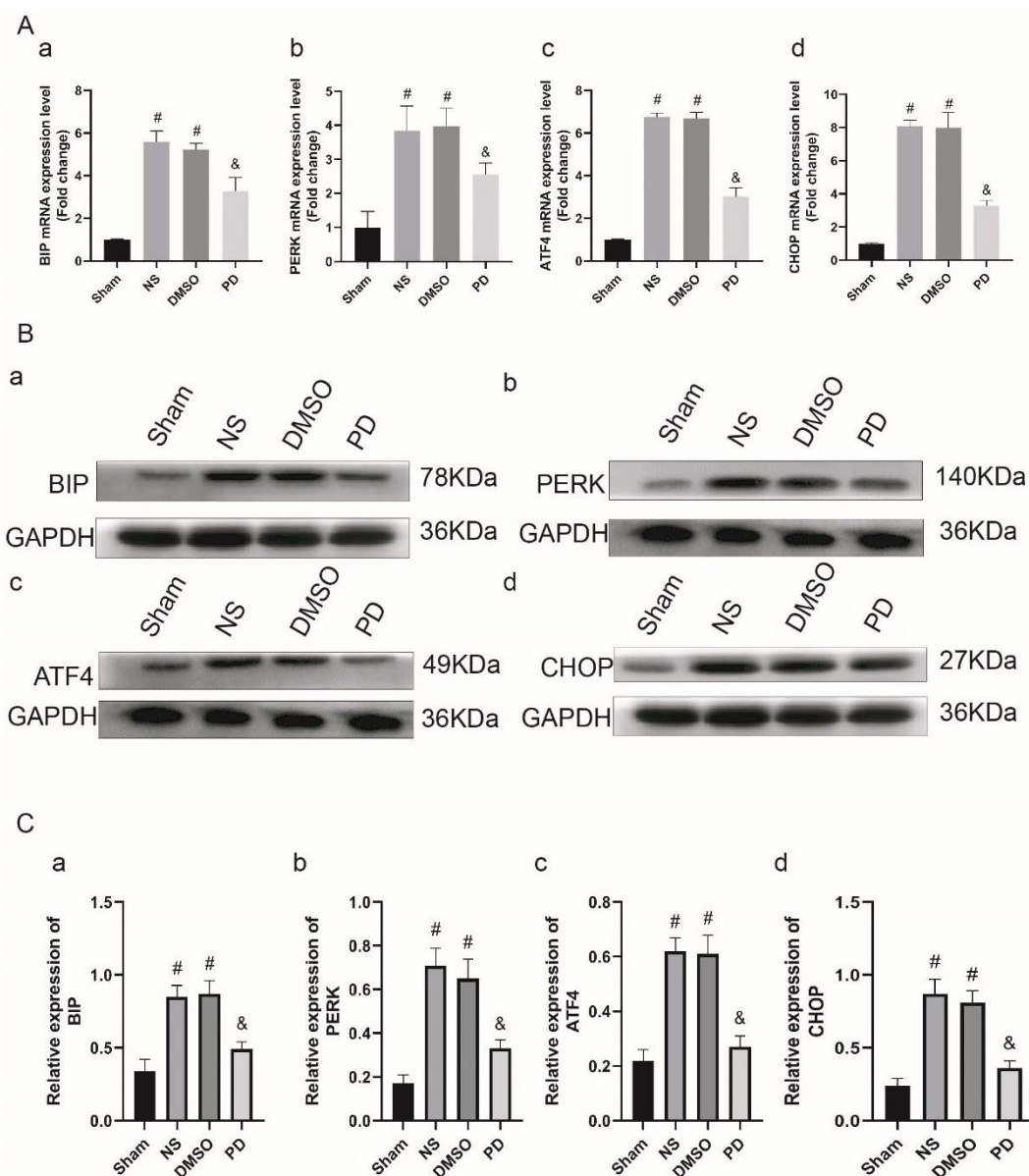
Figure 3 Inhibition of ERK by PD98059 downregulated ERs in the cortices of rat at 24 h after reperfusion. (A)

mRNA expression of (A-a) BIP, (A-b) PERK, (A-c) ATF4 and (A-d) CHOP. (B) WB bands of (B-a) BIP, (B-b) PERK,

(B-c) ATF4 and (B-d) CHOP. Sham, Sham-operated group; NS, saline group; DMSO, dimethyl sulfoxide group; PD,

PD98059 group. (C) The bands intensity analysis of (C-a) BIP, (C-b) PERK, (C-c) ATF4 and (C-d) CHOP. The

mRNA level was assessed by real-time RT -PCR and expressed as the mean ± SD. The values of band intensity were

quantified by ImageJ 6.0 software and expressed as the mean ± SD. #, $P < 0.05$ compared with the Sham group; &,

$P < 0.05$ compared with the DMSO group.

4. Discussion

Previously we manifested that inhibition of ERK with PD98059 had a neuroprotective effect via decreasing oxidative stress, mitochondrial-mediated apoptosis and autophagy in CIRI after CA/CPR [13,14]. However, the effect of ERK inhibition on ERs-induced apoptosis remains unknown. In this study, we utilized the same CA/CPR rat model as in the prior experiments to investigate whether ERs-induced apoptosis participates in the neuroprotection of ERK inhibition. In line with our previous studies, we reconfirmed the neuroprotective effect of ERK inhibition in the CA/CPR rat model by demonstrating the improvement of survival rate, NDS and Nissl bodies in neurons. Moreover, we revealed that inhibition of ERK by PD98059 alleviates ERs-induced apoptosis via downregulation of PERK-ATF4-CHOP pathway after CIRI in the CA/CPR rat model.

ERs apoptotic pathway has been widely studied. PERK-ATF4-CHOP pathway promotes cell apoptosis via inhibition of anti-apoptotic factor B-cell lymphoma-2 (Bcl-2) and activates proapoptotic factor p53 upregulated modulator of apoptosis (PUMA) and tribbles homolog 3 (TRB3). These events finally lead to the initiation of caspase cascade and apoptosis [6]. ERs-induced apoptosis aggravates cell death in CIRI. Wu et al. showed that the GRP78-eIF2α-ATF4-CHOP signaling pathway is activated in rat primary cortical neurons after oxygen glucose deprivation/reoxygenation (OGD/R), while Clausenamide significantly attenuates the ERs-related proteins, reduces apoptosis rate and improves the cellular viability, moreover, its neuroprotection is abolished by the ERs inducer Tunicamycin [17]. As

a member of MAPK family, ERK is involved in the regulation of ERs-induced apoptosis. Yang et al. reported that ERs-induced apoptosis is inhibited by resina draconis via regulating ERK in myocardial IRI, while inhibition of ERK by miR-423-3p suppresses BIP and CHOP, decreases pro-apoptotic protein Bax (Bcl-2 associated X protein), elevates anti-apoptotic protein Bcl-2 [12]. Administration with ERK inhibitor or knockdown with siRNA reverses αNF-induced increment of CHOP and cell apoptosis in HT22 hippocampal neuronal cells [11]. Similarly, our results showed that the cerebral apoptosis index and the expression levels of ERs-related proteins BIP, PERK, ATF4 and CHOP were significantly increased after CIRI. ERK inhibitor PD98059 obviously reduces apoptosis and excessive ERs, improves survival rate, neurological function and protects neurons from CIRI (as shown in Figure 4). Thus, inhibition of ERs-induced apoptosis is possibly involved in the neuroprotective mechanisms of ERK inhibition in CIRI.
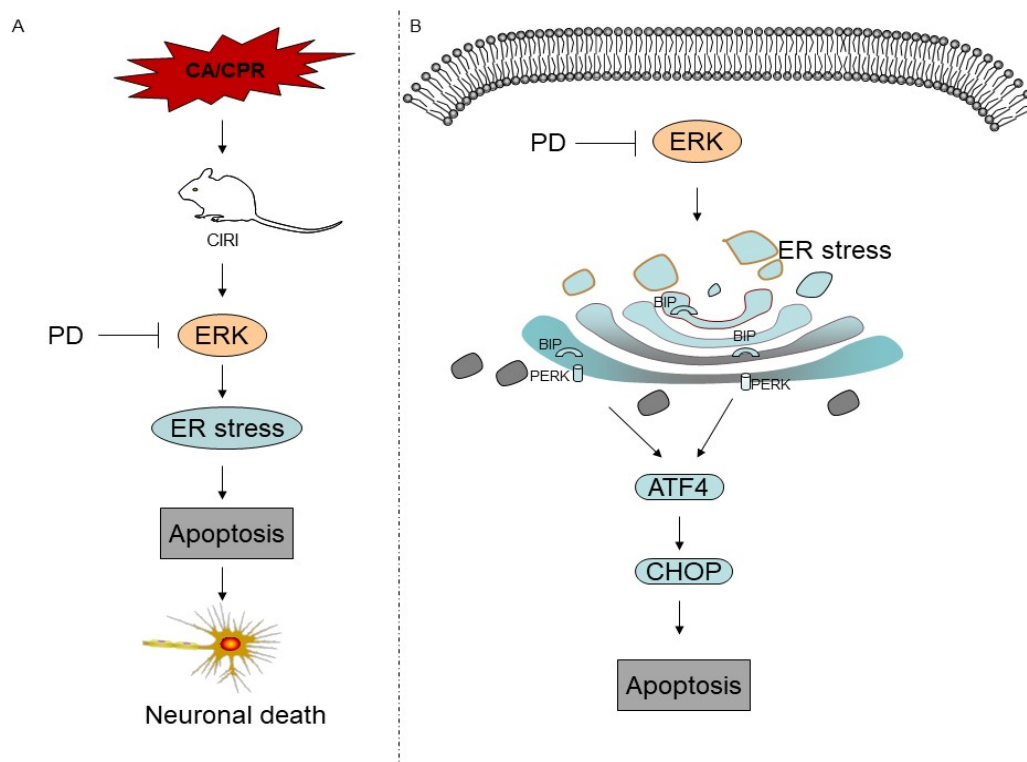
Figure 4 Schematic diagram depicting the pathway involved in CIRI after CA/CPR. (A). CA/CPR-induced CIRI leads to neuronal apoptosis through ERK-ERs pathway; (B). The ERK activates ERs-induced apoptosis via BIP-PERK-ATF4-CHOP pathway. PD98059 inhibit the activation of ERK, thus, suppressing excessive ERs-induced neuronal apoptosis and death. CA, cardiac arrest; CPR, cardiopulmonary resuscitation; CIRI, cerebral ischemia-reperfusion injury; ERK, extracellular signal-regulated kinase; PD, PD98059; ERs, endoplasmic reticulum stress; BIP, binding of chaperone binding immunoglobulin protein; PERK, protein kinase RNA-like ER kinase; ATF4, activated transcription factor 4; CHOP, C/EBP Homologous Protein.

The associations between ERs-induced apoptosis and reactive oxygen species (ROS) is demonstrated by substantial evidences [18,19]. The overproduction of ROS produced in CIRI leads to apoptosis and brain injury [20], which is possibly related to ERs. Study revealed that ROS transfers into ER lumen and damages the tertiary/quaternary structure of protein, leading to the accumulation of misfolded

proteins [21]. Besides, the excessive ROS produced in reperfusion aggravates the depletion of calcium in ER and disturbs protein folding [22]. Both events trig ERs. Furthermore, ROS can also be induced in the process of protein folding and aggravates the oxidative stress within ER [23]. Therefore, ROS and ERs may accentuate each other in a positive feedback mechanism, which activates proapoptotic signaling. Our previous research indicated that ROS significantly increased in brain after CA/CPR, while PD98059 provides the neuroprotection through antioxidant stress as evidenced by markedly decreased ROS and increased superoxide dismutase [13]. Therefore, it is conceivable to infer that ERK inhibition possibly downregulates ERs-induced apoptosis via reduction of ROS and breaking the vicious positive feedback loop between ROS and ERs in CIRI.

ERs-induced apoptosis is closely associated with mitochondrial dysfunction. The contact sites of ER membrane cover nearly 5% of mitochondrial surface to exchange signals and regulate mitochondrial fission/fusion [24]. Phosphorylation of PERK was observed much earlier than the release of cytochrome c in CIRI, indicating that ERs precedes mitochondrial apoptotic pathway [25]. Overactivated PERK upregulates the expression of phorbol-12-myristate-13-acetate-induced protein 1 (Noxa), which increases the mitochondrial permeability and mitochondrial apoptotic signaling via transferring Bax to outer membrane of mitochondria [26]. In our prior study, we observed that PD98059 decreases apoptosis through mitochondrial pathway as confirmed by reversing the mitochondrial permeability transition pore (mPTP) opening, cytochrome c release [14]. Based on the above reports, we suggested that downregulation of ERs by

PD98059 at least partly improves the mitochondrial function and mitigates the development of mitochondrial apoptotic pathway in CIRI.

As a process of self-degradation, autophagy removes proteins and organelles depending on lysosome pathway. Overactivated or dysregulated autophagy is harmful to cell survival [27]. Autophagy-trigged neuronal death is a major consequence of ERs [28]. PERK pathway participates in ERs-induced autophagy. Kouroku et al. verified that dominant negative mutation of PERK prevents autophagy through blunting the conversion of LC3I to LC3II [29]. As a downstream factor of ERs-induced apoptosis, CHOP regulates the death-associated protein kinase 1 (DAPK1), which phosphorylate Beclin1 and detaches it from Bcl-2 to promotes autophagosomes formation [30]. ERs inducer Tunicamycin enhances OGD/R-induced autophagy and decreases cell viability in primary rat cortical neurons after CIRI [31]. Our prior study revealed that the neuroprotection of PD98059 is associated with the downregulation of autophagy as verified by decreased autophagosomes and expression of LC3II, Beclin-1 and increased p62 in CIRI [14]. Combining with our present study, we speculated that autophagy is involved in the ERs-induced cell death in CIRI after CA/CPR.

Our study has several potential limitations. First, it is a preliminary study of ERK inhibitor PD98059 on the ERs and apoptosis, further activation/inhibition of ERs control examines are needed to clarify whether the neuroprotection of ERK inhibition is ERs-dependent in CIRI. Second, considering the PERK-ATF4 is the predominant pathway among the three branches for CHOP activation in ERs, we only detected it without evaluating the other two pathways. Further experiments are under way to

wholly elucidate the role of ERs-induced apoptosis pathway in CIRI after CA/CPR.

In summary, our study reveals that inhibition of ERK by PD98059 alleviates ERs-induced apoptosis via downregulation of PERK-ATF4-CHOP signaling pathway and mitigates CIRI in the CA/CPR rat model.

Acknowledgements

References

1. Panchal AR, Berg KM, Hirsch KG, Kudenchuk PJ, Del Rios M, Cabanas JG, Link MS, Kurz MC, Chan PS, Morley PT, Hazinski MF, Donnino MW. 2019 American Heart Association Focused Update on Advanced Cardiovascular Life Support: Use of Advanced Airways, Vasopressors, and Extracorporeal Cardiopulmonary Resuscitation During Cardiac Arrest: An Update to the American Heart Association Guidelines for Cardiopulmonary Resuscitation and Emergency Cardiovascular Care. *CIRCULATION*. Dec 10 2019;140(24):e881-e894.
2. Babu FS, Majetschak M. Linopirdine-supplemented resuscitation fluids reduce mortality in a model of ischemia-reperfusion injury induced acute respiratory distress syndrome. *Physiol Res*. Aug 31 2021;70(4):649-953.
3. Samakova A, Gazova A, Sabova N, Valaskova S, Jurikova M, Kyselovic J. The PI3k/Akt pathway is associated with angiogenesis, oxidative stress and survival of mesenchymal stem cells in pathophysiologic condition in ischemia. *Physiol Res*. Nov 30 2019;68(Suppl 2):S131-s138.
4. Hetz C, Saxena S. ER stress and the unfolded protein response in neurodegeneration. *Nature Reviews Neurology*. 2017;13(8):477-491.
5. Liu Z, Fei B, Du X, Dai Y, She W. Differential Levels of Endoplasmic Reticulum Stress in Peripheral Blood Mononuclear Cells from Patients with Sudden Sensorineural

Hearing Loss. *Med Sci Monit*. Nov 10 2020;26:e927328.

6. Gorman AM, Healy SJ, Jäger R, Samali A. Stress management at the ER: regulators of ER stress-induced apoptosis. *Pharmacol Ther*. Jun 2012;134(3):306-316.

7. Fels DR, Koumenis C. The PERK/eIF2alpha/ATF4 module of the UPR in hypoxia resistance and tumor growth. *Cancer Biol Ther*. Jul 2006;5(7):723-728.

8. Zhao X, Zhu L, Liu D, Chi T, Ji X, Liu P, Yang X, Tian X, Zou L. Sigma-1 receptor protects against endoplasmic reticulum stress-mediated apoptosis in mice with cerebral ischemia/reperfusion injury. *APOPTOSIS*. Feb 2019;24(1-2):157-167.

9. Cheng L, Li Y, Yao Y, Jin X, Ying H, Xu B, Xu J. Toxic effects of thioacetamide-induced femoral damage in New Zealand white rabbits by activating the p38/ERK signaling pathway. *Physiol Res*. Apr 11 2022;

10. Yu SM, Choi YJ, Kim SJ. PEP-1-glutaredoxin-1 induces dedifferentiation of rabbit articular chondrocytes by the endoplasmic reticulum stress-dependent ERK-1/2 pathway and the endoplasmic reticulum stress-independent p38 kinase and PI-3 kinase pathways. *Int J Biol Macromol*. May 2018;111:1059-1066.

11. Yu AR, Jeong YJ, Hwang CY, Yoon KS, Choe W, Ha J, Kim SS, Pak YK, Yeo EJ, Kang I. Alpha-naphthoflavone induces apoptosis through endoplasmic reticulum stress via c-Src-, ROS-, MAPKs-, and arylhydrocarbon receptor-dependent pathways in HT22 hippocampal neuronal cells. *NEUROTOXICOLOGY*. Mar 2019;71:39-51.

12. Yang T-R, Zhang T, Mu N-H, Ruan L-B, Duan J-L, Zhang R-P, Miao Y-B. Resina draconis inhibits the endoplasmic-reticulum-induced apoptosis of myocardial cells via regulating miR-423-3p/ERK signaling pathway in a tree shrew myocardial ischemia–reperfusion model. *JOURNAL OF BIOSCIENCES*. 2019;44(2):53.

13. Nguyen Thi PA, Chen MH, Li N, Zhuo XJ, Xie L. PD98059 Protects Brain against Cells Death Resulting from ROS/ERK Activation in a Cardiac Arrest Rat Model. *Oxid Med Cell Longev*. 2016;2016:3723762.

14. Zheng JH, Xie L, Li N, Fu ZY, Tan XF, Tao R, Qin T, Chen MH. PD98059 protects the brain against mitochondrial-mediated apoptosis and autophagy in a cardiac arrest rat model. *Life Sci*. Sep 1 2019;232:116618.

15. Chen MH, Liu TW, Xie L, Song FQ, He T, Zeng ZY, Mo SR. A simpler cardiac arrest model in rats. *Am J Emerg Med*. Jul 2007;25(6):623-630.

16. Jia X, Koenig MA, Shin HC, Zhen G, Pardo CA, Hanley DF, Thakor NV, Geocadin RG. Improving neurological outcomes post-cardiac arrest in a rat model: immediate hypothermia and quantitative EEG monitoring. *RESUSCITATION*. Mar 2008;76(3):431-442.

17. Wu F, Zhang R, Feng Q, Cheng H, Xue J, Chen J. (-)-Clausenamide alleviated ER stress and apoptosis induced by OGD/R in primary neuron cultures. *Neurol Res*. Sep 2020;42(9):730-738.

18. Chen Q, Allegood JC, Thompson J, Toldo S, Lesnefsky EJ. Increased Mitochondrial ROS Generation from Complex III Causes Mitochondrial Damage and Increases Endoplasmic Reticulum Stress. *FASEB JOURNAL*. Apr 2019;33(S1):543.13.

19. Sciarretta S, Zhai P, Shao D, Zablocki D, Nagarajan N, Terada LS, Volpe M, Sadoshima J. Activation of NADPH oxidase 4 in the endoplasmic reticulum promotes cardiomyocyte autophagy and survival during energy stress through the protein kinase RNA-activated-like endoplasmic reticulum kinase/eukaryotic initiation factor

2α/activating transcription factor 4 pathway. *Circ Res*. Nov 8 2013;113(11):1253-1264.

20. Hardeland R. Antioxidative protection by melatonin: multiplicity of mechanisms from radical detoxification to radical avoidance. *ENDOCRINE*. Jul 2005;27(2):119-130.

21. Astakhova TM, Morozov AV, Erokhov PA, Mikhailovskaya MI, Akopov SB, Chupikova NI, Safarov RR, Sharova NP. Combined Effect of Bortezomib and Menadione Sodium Bisulfite on Proteasomes of Tumor Cells: The Dramatic Decrease of Bortezomib Toxicity in a Preclinical Trial. *Cancers (Basel)*. Sep 25 2018;10(10):351.

22. Paschen W, Doutheil J. Disturbances of the functioning of endoplasmic reticulum: a key mechanism underlying neuronal cell injury? *J Cereb Blood Flow Metab*. Jan 1999;19(1):1-18.

23. Zeeshan HM, Lee GH, Kim HR, Chae HJ. Endoplasmic Reticulum Stress and Associated ROS. *Int J Mol Sci*. Mar 2 2016;17(3):327.

24. Phillips MJ, Voeltz GK. Structure and function of ER membrane contact sites with other organelles. *Nat Rev Mol Cell Biol*. Feb 2016;17(2):69-82.

25. Häcki J, Egger L, Monney L, Conus S, Rossé T, Fellay I, Borner C. Apoptotic crosstalk between the endoplasmic reticulum and mitochondria controlled by Bcl-2. *ONCOGENE*. May 4 2000;19(19):2286-2295.

26. Zhang L, Lopez H, George NM, Liu X, Pang X, Luo X. Selective involvement of BH3-only proteins and differential targets of Noxa in diverse apoptotic pathways. *Cell Death & Differentiation*. 2010;18(5):864-873.

27. Jiang XM, Hu JH, Wang LL, Ma C, Wang X, Liu XL. Ulinastatin alleviates neurological deficiencies evoked by transient cerebral ischemia via improving autophagy, Nrf-2-ARE and apoptosis signals in hippocampus. *Physiol Res*. Aug 16 2018;67(4):637-646.

28. Yorimitsu T, Nair U, Yang Z, Klionsky DJ. Endoplasmic reticulum stress triggers autophagy. *J Biol Chem*. Oct 6 2006;281(40):30299-30304.

29. Kouroku Y, Fujita E, Tanida I, Ueno T, Isoai A, Kumagai H, Ogawa S, Kaufman RJ, Kominami E, Momoi T. ER stress (PERK/eIF2alpha phosphorylation) mediates the polyglutamine-induced LC3 conversion, an essential step for autophagy formation. *Cell Death Differ*. Feb 2007;14(2):230-239.

30. Qi Z, Chen L. Endoplasmic Reticulum Stress and Autophagy. *Autophagy: Biology and Diseases*. 2019:167-177:chap Chapter 8. *Advances in Experimental Medicine and Biology*.

31. Ma X, Zhang W, Xu C, Zhang S, Zhao J, Pan Q, Wang Z. Nucleotide-binding oligomerization domain protein 1 enhances oxygen-glucose deprivation and reperfusion injury in cortical neurons via activation of endoplasmic reticulum stress-mediated autophagy. *Exp Mol Pathol*. Dec 2020;117:104525.